WILEY | Hindawi

Research Article

Research on Productivity Evaluation Method Based on Shale Gas Well Early Flow Stage Data

Yize Huang [iD],[1,2,3] Xizhe Li [iD],[1,2,3] Wei Guo,[3] Xiaohua Liu,[3] Wei Lin [iD],[4] Chao Qian [iD],[3,5] Mengfei Zhou,[1,2] Yue Cui,[1,2] and Xiaomin Shi[3]

[1]*University of Chinese Academy of Sciences, Beijing 100049, China*
[2]*Institute of Porous Flow & Fluid Mechanics, Chinese Academy of Sciences, Langfang 065007, China*
[3]*PetroChina Research Institute of Petroleum Exploration & Development, Beijing 100083, China*
[4]*School of Geosciences, Yangtze University, Wuhan 430100, China*
[5]*Shale Gas Exploration and Development Department, CNPC Chuanqing Drilling Engineering Co., Ltd., Chengdu, Sichuan 610051, China*

Correspondence should be addressed to Yize Huang; huangyize20@mails.ucas.ac.cn and Xizhe Li; lxz69@petrochina.com.cn

Since the accurate early gas well production regime is related to the production period and final productivity, it is crucial to make better use of early flow stage production data for gas well productivity evaluation. Absolute open flow potential (AOF) and estimated ultimate recovery (EUR) are essential parameters for evaluating the productivity of shale gas wells. This study establishes new AOF calculation methods for the early production stage. The analytical model can calculate the AOF only by using stable pressure and production data in the flowback stage, which greatly improves the efficiency of productivity evaluation. Three methods have, respectively, calculated the productivity of the shale gas wells above 3500 m in the Luzhou block. The results show that well L2-3 has the highest AOF, averaging 278.1×10^4 m³/d, whereas well Y2-8 has the lowest AOF, averaging 100.2×10^4 m³/d. Different AOF calculation methods are identified for gas wells in different stages of production. For gas wells in the initial unstable flow stage, a pseudogas production index method is recommended. A water production index analysis method, with lower evaluation results, is proposed for gas wells in the flowback stage. A modern production decline analysis method is found to be preferred for calculating the EUR of deep shale gas wells. Well L2-3 has the highest average EUR of 1.26×10^8 m³, whereas well Y2-8 has the lowest average EUR of 0.42×10^8 m³. The Blasingame method is recommended for medium-to-high-production gas wells, whereas a normalized pressure integral method is suggested for low-production wells. A strong exponential quantitative link between the AOF and the EUR shows that a fracture system's initial productivity has a significant impact on a well's EUR. The findings of this study enrich the productivity evaluation system, increase the accuracy of productivity evaluation results, and provide theoretical support for deep shale gas wells.

1. Introduction

Shale gas is an unconventional energy source with high development potential [1–3]. However, the reservoir of natural fractures and the cross-scale flow mechanism created by artificial fracturing have led to the production features of high peak production and decline rate. Shale has the characteristics of ultra-low porosity and permeability [4]. Geological and engineering factors have caused shale gas wells to be in an unstable flow stage for a long time, making productivity evaluation particularly difficult. Productivity evaluation is the most important approach for monitoring well dynamics, predicting well productivity, calculating reservoir parameters, and evaluating fracturing effects in the development process of gas wells [5]. Establishing a suitable controlled pressure and production system at an early stage of development becomes especially valuable in order to obtain high gas production with lengthy production periods under such complex geological conditions.

The AOF and EUR in the early stage play an essential role in the production regime [6].

The productivity of a gas well in conventional gas reservoirs is typically evaluated using the absolute open flow potential (AOF) as an evaluation index, which is the gas production when the flow pressure at the bottom of the well is zero. It can be obtained by analyzing test data using the productivity well test method [7]. The adsorbed and free gas within the shale matrix are not taken into account by the AOF in the test gas stage, which only accounts for productivity within the reservoir-reformed zone. Therefore, the estimated ultimate recovery (EUR) has become another mainstream evaluation index.

Currently, the methods for evaluating shale gas well productivity are classified as follows: production decline analysis method, analytical method, numerical simulation method, and machine learning method. Many scholars proposed various empirical formulas and derivative methods [8–11] for analyzing the production decline of a single well under constant pressure production conditions, such as Arps, PLE, SEPD, and YM-SEPD [12–18]. The production decline analysis method has been expanded by introducing the material balance pseudotime and normalized pseudopressure functions [19–25], which have been widely used in the productivity evaluation of tight gas reservoirs such as shale gas, as the analysis object has been extended from a single gas well production analysis to a two-parameter analysis of production and pressure [26–31]. However, the limitations of applying the production decline method for shale gas flow stages have also caused some uncertainties in the productivity evaluation results [32–34].

As research scholars continue to study shale gas transport laws in the subsurface, the analytical method of productivity evaluation can better describe the flow mechanisms in different stages of shale gas development [35–39]. By using the mass transfer control equation, which takes into account the existence of distinct flow mechanisms like the Knudsen diffusion [40–45], molecular surface diffusion, adsorption-desorption, the Klinkenberg effect, the high-speed non-Darcy effect, Darcy flow, and the effective stress sensitivity of shale gas in the reservoirs [46–55], an analytical model describing the cross-scale transport of molecules is created. However, due to the many idealized assumptions in the analytical model, the analytical method cannot accurately reflect the complex flow mechanisms and development laws of shale gas in the actual formation [56–58]. With the continuous integration of the artificial intelligence with oil and gas field production sites, machine learning methods are gradually emphasized in the productivity evaluation of shale gas wells [59–62].

However, shale gas has distinct geological properties, complex flow mechanisms, advanced reservoir reforming technologies, and preferred gas well production methods; the productivity index is affected by both engineering and geological considerations [63–65]. Thus, accurate results are not easily obtained [66–68]. Therefore, establishing a new and accurate productivity evaluation method for deep shale gas wells is the focus of the current research in shale gas reservoir engineering. Conventional productivity test methods mainly include back pressure tests (BPTs), isochronal tests, and modified isochronal tests. A productivity equation is fitted to stable pressure and production data obtained from multiple production systems, and the AOF is calculated by combining the productivity curve. On the one hand, verifying the results is difficult because the AOF is the ultimate production of gas wells [69, 70]. Although the production data used in these methods is readily available, a period of decline in gas well production is required before the EUR evaluation, and there is a time lag. The complex flow mechanism of shale gas leads to underfitting, and multiple fitting parameters yield multiple solutions [71, 72]. An analytical method requires detailed geological parameters of the gas reservoir, a transfer equation can describe the cross-scale flow mechanism of shale gas, and analytical solutions of production can be obtained using the Laplace transform and Green's function [73–75]. However, a model for an analytical method is established with many idealized assumptions, which cannot accurately reflect the actual flow of shale gas in a subsurface reservoir. These errors can significantly affect the accuracy of productivity evaluation [76, 77]. Briefly, there are still many challenges in the current research on shale gas well productivity evaluation.

In summary, owing to geological and engineering factors, shale gas wells have been in the early unstable flow and flowback stages for a long time [78]. In this study, a pseudogas production index method and a water production index analysis method are constructed in order to produce more accurate results for gas well productivity evaluation utilizing the production data in these stages and to decrease their delay. The core principles of production decline analysis (PDA) are defined concurrently in order to enhance the shale gas well productivity evaluation system and get reliable productivity forecast indices. The calculation results and application prospects of each method are examined using three shale gas wells from the Luzhou block of the Sichuan Basin of China as examples. The research results are expected to provide theoretical support for methods for evaluating shale gas well productivity as well as scientific guidance for the formulation of development technology policies.

2. Theory of Productivity Evaluation Method of Deep Shale Gas Well

2.1. Empirical Method.
The traditional AOF calculation method makes reference to test well analysis of production data utilizing a BPT method. Exponential, binomial, and one-point procedures make up the majority of BPT techniques [7].

The exponential equation is an empirical relationship between the gas well production and the constant flow pressure proposed by Rawlins in 1936 [6], which is expressed in

$$q_g = C\left(p_R^2 - p_{wf}^2\right)^n. \tag{1}$$

Logarithms of the two sides of Equation (1) are taken to

yield

$$\lg q_g = \lg C + n \lg \left(p_R^2 - p_{wf}^2\right), \tag{2}$$

$$\lg \left(p_R^2 - p_{wf}^2\right) = \frac{1}{n} \lg q_g - \frac{1}{n} \lg C. \tag{3}$$

From Equation (3), it can be interpreted that $\left(p_R^2 - p_{wf}^2\right)^n$ and q_g are linearly related on a bilogarithmic plot with a slope of $1/n$ and an intercept of $-1/n \lg C$. The line represents the exponential productivity curve.

Using a BPT to obtain the constant production and pressure, an exponential capacity curve can be easily drawn, the slope of which provides the value of n; C can be obtained from

$$C = \frac{q_g}{\left(p_R^2 - p_{wf}^2\right)^n}. \tag{4}$$

At $p_{wf} = 0$, substituting the initial reservoir pressure, p_R, into Equation (5) yields q_{AOF} of the gas well.

$$q_{AOF} = C\left(p_R^2\right)^n, \tag{5}$$

where q_g is the gas production ($10^4 \, m^3/d$), p_R is the initial reservoir pressure (MPa), p_{wf} is the flow pressure at the bottom of the well (MPa), C is the productivity equation coefficient ($10^4 \, m^3/d/MPa^{2n}$), and n is the seepage index.

2.2. Pseudogas Production Index Method. Production data from deep shale gas wells are characterized by early and rapidly declining and long-term unstable flow stages, making it difficult to reach the quasistable flow stage [77, 78]. When a well is in the unstable flow stage, its pseudogas production index versus material balance time bilogarithmic plot is a straight line with a slope of 0 to $-1/2$ [69, 70]. The production data of wells in the unstable flow stage are fit to a straight-line section to obtain the early pseudogas production index. The main benefit of the pseudogas production index approach over the traditional method is that it broadens the application conditions by calculating AOF without requiring production to reach the quasistable flow stage and providing future prediction findings. The pseudogas production index is defined in

$$\frac{q_g}{\Delta m(p)} = \frac{q_g}{m(p_i) - m(p_{wf})}, \tag{6}$$

$$m(p_k) = 2 \int_0^p \frac{p_k}{\mu u_{gk} Z_k} dp. \tag{7}$$

According to Sun et al., the early-stage pressure meets the conditions for using the p^2 method, assuming that μZ is a constant. Therefore, p^2 is used to substitute $m(p)$ [79].

The material balance time is defined in

$$t_m = \frac{N_p}{q_g}. \tag{8}$$

The pseudogas production index for the first day is obtained by fitting a straight-line section to the early unstable flow stage data, and the results are substituted into Equation (9) to calculate the AOF.

$$q_{AOF} = \frac{q_g}{\Delta m\left(p_{tmb_{early}}\right)} m(p_i), \tag{9}$$

where $k = i$ or wf, $m(p_k)$ is the pseudopressure when the pressure is p_k ($MPa^2/(mPa\,s)$), μ_{gk} is the gas viscosity when the pressure is p_k (mPa s), Z_k is the gas deviation factor when the reservoir pressure is p_k, N_p is the cumulative production (m^3), and t_m is the material balance time (t).

The lack of test production from shale gas wells in a block makes early productivity evaluation difficult [3]. Therefore, this study establishes a pseudogas production index method to calculate the AOF based on the analysis of production data in the early unstable flow stage. However, because this method requires gas well production data, it is applicable to deep shale gas wells in the early unstable flow stage.

2.3. Flowback Water Production Index of Analytical Method. Fracturing fluid flowback is performed after the completion of gas well fracturing. A shale gas well's hydraulic fracture flowback model is shown in Figure 1. After hydraulic fracturing, the well is saturated, and the fracturing fluid then flows from the microfracture into the main fracture and finally into the wellbore to the surface. h is the fracture height, w is the fracture width, and n is the number of fractures. The flowback rates of shale gas wells worldwide are low, only 10%–40%, among which those of deeper shale gas wells are relatively higher [79, 80]. For a nonflowback fracturing fluid, the following are generally accepted:

(1) A fracturing fluid enters the micropores in the matrix because of imbibition

(2) A fracturing fluid is retained in fractures that rapidly close within a short period

In this study, water is considered to constitute a large proportion of a fracturing fluid and used to represent it. The variations in the pressure, water production, and gas production with time are shown in Figure 2. In the early stage (Figure 2(a)), the mobile fluid in the fracture system is single-phase water, gas production is not seen, the pressure progressively changes, and the cumulative water production rises, signifying an unstable flow stage. In the middle stage (Figure 2(b)), the gas production in the fracture system gradually increases, and both the pressure and water production reach a peak. The water in one part of the fracture is still in the unstable flow stage, whereas the water in the other part of the fracture enters the pseudostable flow stage. The gas starts to break through into the fracture, and this stage belongs to the transition flow stage.

When pressure reaches the fracture barrier in the latter stage (Figure 2(c)), the entire fracture system appears to be in a two-phase flow. The water in the matrix is difficult to flowback because of the imbibition effect, and at this point, if
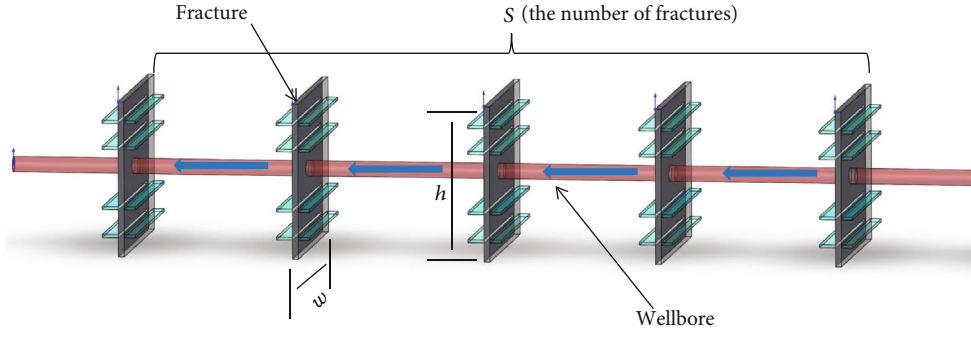
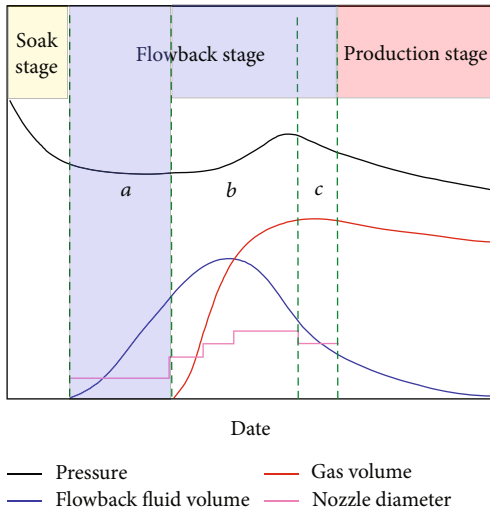FIGURE 1: Hydraulic fracture flowback model of shale gas well.

FIGURE 2: Flowback and production characteristic curves of shale gas well.

there is no energy supplement from the reservoir, the flow is anticipated to enter the suggested stable flow stage [81, 82].

Based on the flowback characteristics of the Luzhou deep shale gas wells, the flowback water production index of analytical method is based on the data of stage a in Figure 2. Stage a is in the early stage of gas well flowback. After a period of well soak, a large amount of fracturing fluid and movable water is discharged from the fracture. At this stage, it is assumed that no gas is produced. The water in the matrix-fracture system is assumed to behave as a bilinear flow. The analytical model for the flowback stage is established as expressed in Equation (10), and the boundary conditions within the model correspond to constant production. The model assumptions and the detailed derivation process are presented in Appendix A.

$$\begin{cases} \dfrac{\partial^2 p}{\partial x^2} = \dfrac{\varphi \mu c_t}{0.0853k} \dfrac{\partial p}{\partial t}, \\ p(x,0) = p_i, \\ \left(\dfrac{\partial p}{\partial x}\right)_{x \to 0} = \dfrac{q_w B \mu}{0.0853khwn}, \\ p(\infty,t) = p_i. \end{cases} \tag{10}$$

Solving Equation (10) yields the following relationship between water production and pressure:

$$q_w = \frac{nhw(p_i - p_{wf})}{2B_w} \sqrt{\frac{0.0853\pi k\varphi c_t}{t\mu_w}}. \tag{11}$$

Using the same approach and assuming that the fluid in the matrix-fracture system during the production stage is a single-phase gas, an analytical bilinear flow model for gas production during the production stage is expressed in

$$\begin{cases} \dfrac{\partial^2 m(p)}{\partial x^2} = \dfrac{\varphi \mu c_t}{k} \dfrac{\partial m(p)}{\partial t}, \\ m(x,0) = p_i, \\ \left(\dfrac{\partial m}{\partial x}\right)_{x \to 0} = \dfrac{q_g \mu p_{sc} T}{0.0853khwnT_{sc}}, \\ m(\infty,t) = p_i. \end{cases} \tag{12}$$

Solving Equation (12) yields the relationship between gas production and pseudopressure as follows:

$$q_g = \frac{nhw(m(p_i) - m(p_{wf}))T_{sc}}{2p_{sc}TB_g} \sqrt{\frac{0.0853\pi k\varphi c_t}{tu_g}}. \tag{13}$$

The gas well AOF is provided by

$$q_{AOF} = \frac{nhwT_{sc}m(p_i)}{2p_{sc}TB_g} \sqrt{\frac{0.0853\pi k\varphi c_t}{t\mu_g}}. \tag{14}$$

By combining Equations (11) and (14), the formula for calculating the AOF following simplification is expressed in

$$\frac{q_{AOF}}{q_w} = \frac{T_{sc}B_w m(p_i)\sqrt{\mu_w}}{p_{sc}TB_g(p_i - p_{wf})\sqrt{\mu_g}}. \tag{15}$$

TABLE 1: Summary of production decline analysis methods.

| Method category	Method subcategory	Applicable conditions	Advantages/disadvantages
Arps	Exponential decline curve Harmonic decline curve Hyperbolic decline curve	Quasistable flow/single well/ constant pressure production system	Underfitting with data in early decline stage/high productivity prediction result
Fetkovich	Theoretical plate method of normalized decline curve fitting		Total production data fitting/constant pressure only
New empirical model	PLED SEPD Duong Improved hyperbolic decline	Unstable flow/quasistable flow/ single-well/constant-pressure production system	Entire production data fitting/uncertainty of prediction results is high when production data are few
Modern PDA model	Blasingame A-G and NPI	Entire production flow/single-well/variable pressure production system	Entire production data fitting/many fitting parameters lead to existence of multiple solutions
Flow material balance	Fitting method of material balance equation for material balance pseudotime function	Quasistable flow/variable pressure production system	Obtain linear relationship to calculate geological reserves in unstable stage
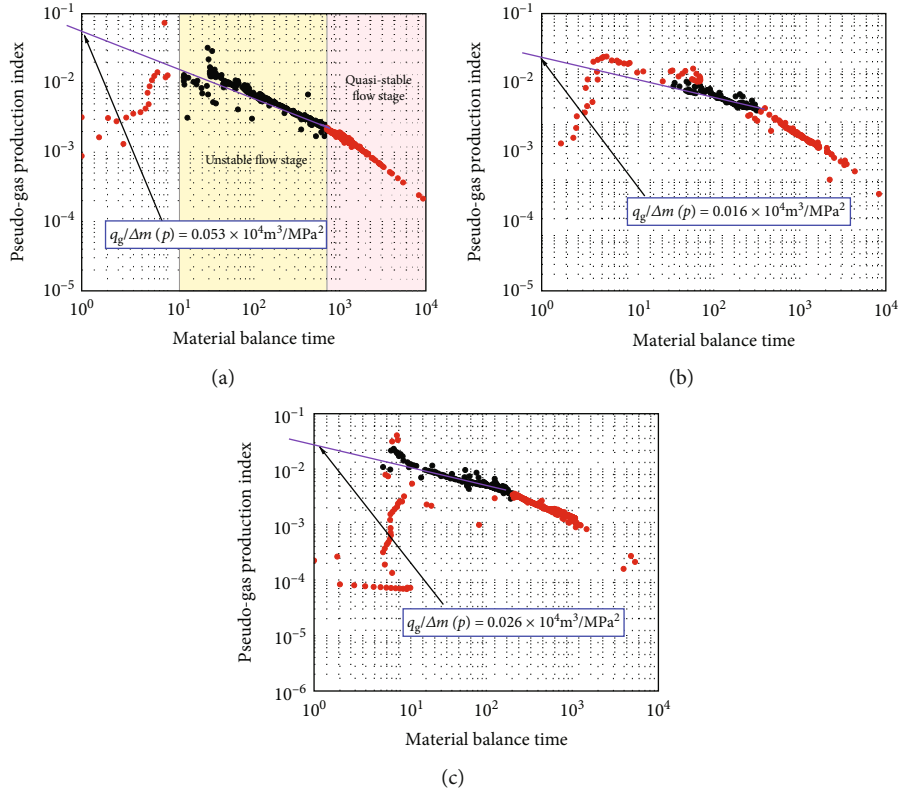
FIGURE 3: Production curves of pseudogas production index method: (a) L2-3, (b) Y2-8, and (c) Y4-5.

TABLE 2: Calculation parameters and results of pseudogas production index method.

Well name	p_i (MPa)	$m(p_i)$ (MPa²/ (mPa s))	$q_g/\Delta m(p)$ (10^4 m³/ d/MPa²)	q_{AOF} (10^4 m³/d)
L2-3	72.00	5184	0.053	274.75
Y2-8	79.00	6241	0.016	99.85
Y4-5	75.00	5625	0.026	146.25

The AOF is calculated using Equation (16) by obtaining the relevant parameters and the values of flowback rate and pressure based on the gas well data.

$$q_{gAOF} = \frac{q_w}{p_i - p_{wf}} \frac{T_{sc}B_w m(p_i)\sqrt{\mu_w}}{p_{sc}TB_g\sqrt{\mu_g}}. \tag{16}$$

In practical applications, the data related to the above equations are difficult to obtain accurately and complex to use.
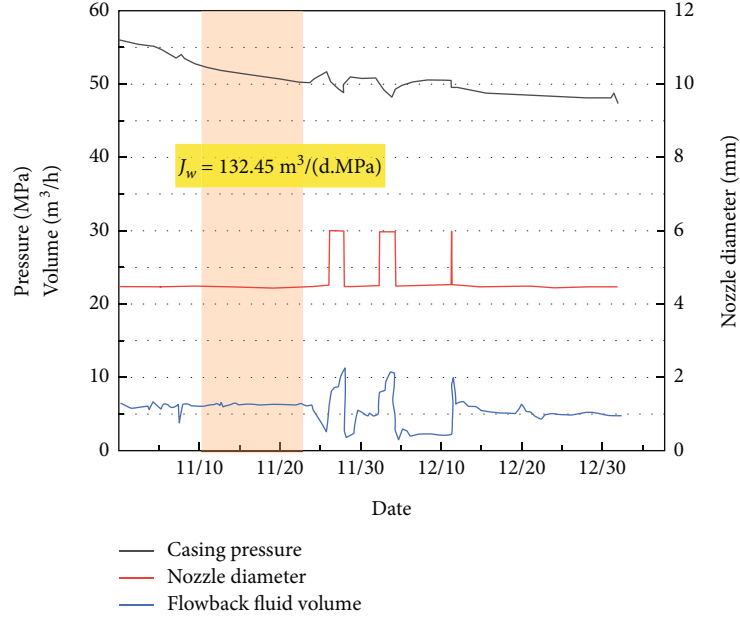
FIGURE 4: Flowback curve of L2-3 well.

TABLE 3: Calculation parameters and results of water production index analytical method.

Well name	Reservoir pressure P_i (MPa)	Temperature (°C)	J_w (m³/d/MPa)	q_{AOF} (10⁴ m³/d)
L2-3	72	138	132.45	262.54
Y2-8	79	145	39.72	90.89
Y4-5	75	140	62.23	132.93

TABLE 4: Calculation parameters and results of empirical method.

Back pressure test	Nozzle diameter (mm)	p_{wf} (MPa)	q_g (10⁴ m³/d)	$p_r^2 - p_{wf}^2$ (MPa²)
Productivity point 1	5	53.60	18.89	1721.444
Productivity point 2	7	52.30	24.29	1859.216
Productivity point 3	10	49.84	31.28	2110.18

Therefore, this study establishes a productivity evaluation method using a water production index. For the curve smoothing part, the relationship between cumulative water production and pressure changes over a specific period of time is determined using the characteristic curve of the shale gas flowback stage. The water production index, J_w, is calculated using the cumulative water volume per unit time and unit pressure.

$$J_w = \frac{Q_w}{(p_i - p_{wf})t}. \tag{17}$$

Equation (17) is substituted into Equation (16), which is simplified as

$$q_{AOF} = J_w \frac{T_{sc} B_w m(p_i) \sqrt{\mu_w}}{p_{sc} T B_g \sqrt{\mu_g}}, \tag{18}$$

where q_w is the water production (m³/d); h is the fracture height (m); w is the fracture length (m); p_i is the initial reservoir pressure (MPa); p_{wf} is the flow pressure at the well bottom (MPa); B_w is the water volume factor, with a value of 1.02; k is the permeability (mD); φ is the porosity (%); c_t is the reservoir compressibility coefficient; μ_w is the water viscosity, with a value of 1.3 mPa·s; q_{AOF} is the AOF (10⁴ m³/d); T_{sc} is the standard state temperature, with a value of 15°C; p_{sc} is the standard state pressure, with a value of 0.101325 MPa; B_g is the gas volume factor, with a value of 3.0×10^{-3} m³/m³; μ_g is the gas viscosity, with a value of 0.0135 mPa·s; and J_w is the water production index.

3. Theory of EUR Evaluation Method of Deep Shale Gas Well

Shale gas EUR evaluation methods include the material balance, PDA empirical, and modern PDA methods. The PDA method does not need to consider a reservoir geological model and a production system and uses only production data; the method has the characteristics of simplicity and practicality. These methods have been developed into mature commercial software (e.g., Harmony) and are the mainstream methods for EUR evaluation. This study describes the basic principles and application conditions of productivity evaluation methods, establishes an EUR evaluation process for deep shale gas wells, and evaluates the EURs of the three shale gas wells in the Luzhou block.
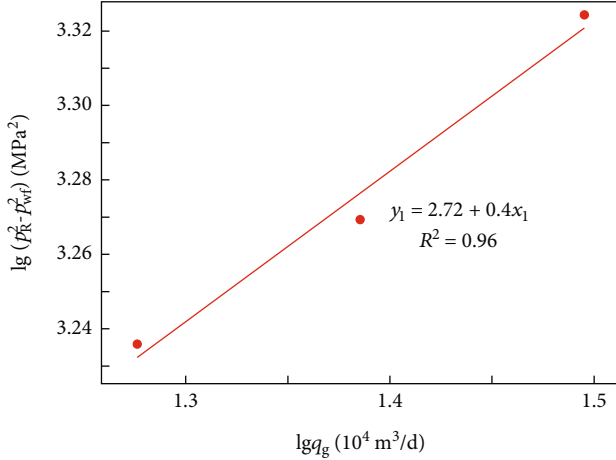
FIGURE 5: Productivity curve of L2-3 using empirical method.

TABLE 5: Calculation parameters of numerical simulation method.

Parameter	Well name		
	L2-3	Y2-8	Y4-5
Drainage area (ha)	152.1	155.30	136.50
Original gas in place (10^6 m^3)	288.13	402.64	297.97
Horizontal length (m)	1560	1853	1751
Facture half length (m)	25	15	30
Temperature (K)	411	418	413
Reservoir pressure (MPa)	72	79	75
Net pay (m)	22	25	20
Total porosity (%)	4.9	4.6	4.5
Initial gas saturation (%)	54	60	61
Permeability (mD)	0.27	0.21	0.19

Gas wells must continuously produce in order for an empirical method to work. An empirical method cannot be used to produce a system with changeable bottom-hole flow pressure [71]. However, most gas wells adopt such a system for actual production. In addition, the actual production process for a single-phase gas well has both variable pressure and production, owing to the compressibility of the gas. For the PDA of gas wells under variable production and pressure conditions, Blasingame et al. and Jieming et al. presented a material balance pseudotime function and a normalized pseudopressure [30, 31]. This is the greatest advantage of modern PDA methods.

The fundamental idea behind this approach is to use a material balance pseudotime parameter to examine the transition of an evaluation object from liquid to gas phases. Using normalized pressure parameters, the pseudopressure flow equation of a gas well is changed into a normalized pseudopressure flow equation. Finally, the application condition of the PDA method is altered from being constant pressure to variable pressure. By simplifying the flow equation and fitting it with actual production data, physical parameters of the actual formation can be obtained, and the gas well productivity can be effectively predicted [32].

The Blasingame method uses the material balance time and a pseudotime function to obtain the material balance pseudotime function and combines the normalized pseudopressure to extend the Fetkovich method.

The pseudotime function of the material balance is defined in

$$t_{ca} = \frac{\mu_{gi} C_{ti}}{q_g} \int_0^t \frac{q_g}{\mu_g C_t} dt. \tag{19}$$

The normalized pseudopressure is defined in

$$p_p = \frac{\mu_{gi} Z}{p_i} \int_0^p \frac{p}{\mu_g Z} dp. \tag{20}$$

The pseudo-pressure-normalized production is defined in

$$\frac{q_g}{\Delta p_p} = \frac{q_g}{p_{pi} - p_{pwf}}, \tag{21}$$

where u_{gi} and u_g are the gas viscosities at pressures p_i and p, respectively (mPa·s); C_{ti} and C_t are the total reservoir compressibility coefficients at pressures p_i and p, respectively (MPa^{-1}); t is the production time (d); t_{ca} is the material balance pseudotime (d); q_g is the gas production (m^3/d); and p_p is the normalized pseudopressure under reservoir conditions p (MPa).

The Blasingame approach uses three characteristic curves to collectively fit the data to compute the EUR in order to improve calculation accuracy and combat result distortion caused by the low precision of the production data. These are the pseudo-pressure-normalized production curve $(q_g/\Delta p_p)$, pseudo-pressure-normalized production integral curve $(q_g/\Delta p_p)_i$, and pseudo-pressure-normalized production derivative curve.

The Agarwal-Gardner (A-G) method and the normalized pressure integral (NPI) method are also the main methods for PDA [33]. Based on the Blasingame decline analysis method, the A-G method adds a dimensionless parameter relationship to unstable well test analysis to establish a PDA-type curve. This type of curve fitting analysis process is the same as the Blasingame method. This method mainly analyzes the production and time relationship data. The distinction between the Blasingame and A-G approaches, which decreases the many solutions of the fitting, is in the definitions of the dimensionless parameters. The dimensionless production of the A-G technique is converted to a dimensionless pressure using the type curve of the NPI method. The horizontal axis of a type curve is still a dimensionless time. The process of the type-curve fitting analysis of the NPI method is similar to those of the other two methods.

In addition to calculating the EUR, modern PDA methods can quantify and analyze other reservoir parameters, such as permeability and skin coefficient [34]. The results of the type-curve fitting are subsequently used to
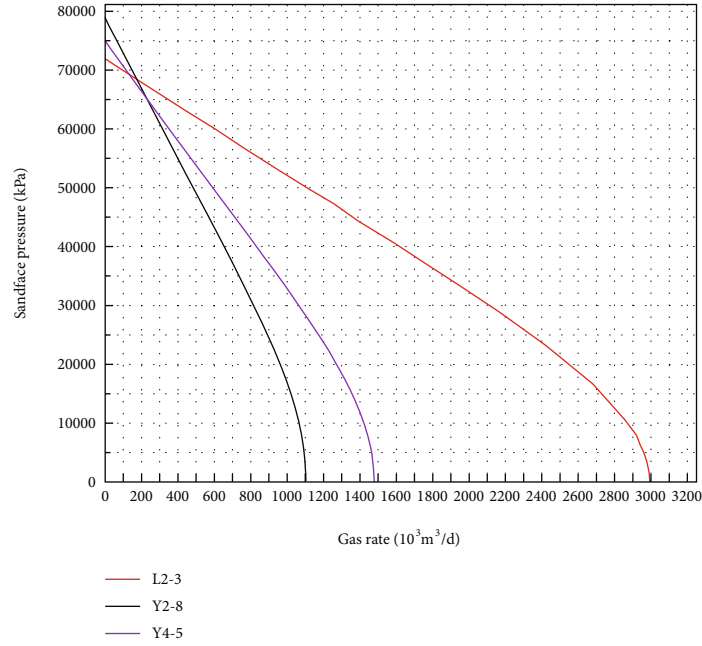
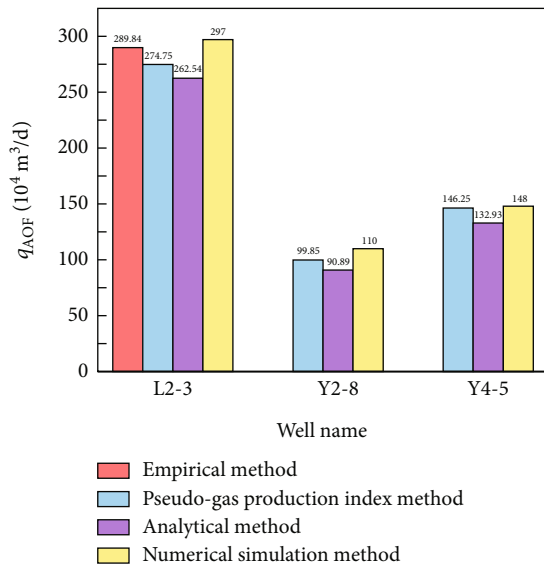FIGURE 6: Numerical simulation results of IPRs of shale gas wells.

FIGURE 7: Comparison results of different calculation methods.

qualitatively identify the gas flow stage and production status of a gas well.

The EUR evaluation methods for shale gas wells are summarized in Table 1.

4. Results and Discussions

4.1. Results of Pseudogas Production Index Method. We evaluated three deep shale gas wells in the Luzhou block—L2-3, Y4-5, and Y2-8—using the established pseudogas production index method.

First, bilogarithmic curves of the pseudogas production index and the material balance time were plotted using the production data of the three gas wells in the unstable flow stage. It is noticeable from Figure 3 that the data points vary regularly over a straight line with a slope of 0 to −1/2. The early pseudogas production index values of the three gas wells were obtained by fitting the intersection of the straight-line section exhibited in the early unsteady flow stage with the vertical coordinate axis.

From Figure 3, the pseudogas production indexes are $0.053 \times 10^4 \, \text{m}^3/\text{d/MPa}^2$ for L2-3, $0.016 \times 10^4 \, \text{m}^3/\text{d/MPa}^2$ for Y2-8, and $0.026 \times 10^4 \, \text{m}^3/\text{d/MPa}^2$ for Y4-5. The measured parameters and pseudogas production indexes of the three gas wells were substituted into Equation (9), and the AOF results were calculated, which are listed in Table 2.

The results in Table 2 suggest that a large productivity gap occurs among the wells, where well L2-3 has the largest AOF of $274.75 \times 10^4 \, \text{m}^3/\text{d}$, whereas well Y2-8 has the lowest AOF of $99.85 \times 10^4 \, \text{m}^3/\text{d}$. This suggests that well L2-3 has better reservoir conditions and a well-developed fracture system than the other two wells, and the initial productivity of this gas well is high.

4.2. Results of Flowback Water Production Index of Analytical Method. The three deep shale gas wells in the Luzhou block were analyzed using the water production index analytical method. Shale gas was produced using a pressure-controlled method during the flowback stage. Therefore, a smooth section of the pressure curve variation was selected, and the water production time, pressure value, and accumulated water production were substituted into Equation (17) to calculate the water production index, J_w. As shown in Figure 4, the water production index, J_w, for well L2-3 is $132.45 \, \text{m}^3/\text{d/MPa}$, and those calculated for the remaining two wells, Y2-8 and Y4-5, are $39.72 \, \text{m}^3/\text{d/MPa}$ and $62.23 \, \text{m}^3/\text{d/MPa}$, respectively.

TABLE 6: Calculation parameters of modern PDA method.

Parameter	Well name		
	L2-3	Y2-8	Y4-5
Wellhead temperature (K)	65	70	65
Sandface temperature (K)	411	418	413
Reservoir pressure (MPa)	72	79	75
Net pay (m)	22	25	20
Total porosity (%)	4.9	4.6	4.5
Measured depth (m)	5600	6100	6260
True vertical depth (m)	3891	4057	4129
Maximum deviation angle (°)	92.6	96.5	93.9
Initial gas saturation (%)	54	60	61
Gas impurity			
CO_2 (%)	1.33	1.46	0.98
H_2S (%)	0	0	0.03
N_2 (%)	0.56	0.56	0.61
Deviation factor (Z)		1.5	
Volume factor (B_g)		3	
Gas viscosity (mPa·s)		0.0135	

The AOFs of the gas wells were calculated using the water production index analytical method, and the results are listed in Table 3. The AOF of well L2-3 is the highest at $262.54 \times 10^4 \text{ m}^3/\text{d}$, whereas that of well Y2-8 is the lowest at $90.89 \times 10^4 \text{ m}^3/\text{d}$. The water production index analytical method only requires stable production data in the flowback stage, to deduce the AOF, and the required data are accurate and easily available, which significantly reduces the calculation cost and avoids the calculation errors caused by irregular data.

4.3. Results of Empirical Method. Conventional BPTs are conducted for shale gas wells, which require that both the wellhead pressure and gas production should be stable for at least 5 days and their fluctuations should not exceed 5%. However, deep shale gas well reservoirs have developed micro-nanopores with extremely low porosity and permeability and no natural productivity. Their complex fracture system must be obtained by a large-scale reservoir fracturing and reforming technology, owing to the industrial gas flow and economic benefits [4]. Currently, many shale gas wells are produced using pressure-controlled methods, which generally fail to obtain the required test pressure and test production. Among the three shale gas wells in the block considered in this study, only well L2-3 met the requirements for a BPT well analysis. An exponential empirical method was used to calculate the AOF. The initial reservoir pressure, p_r, of well L2-3 was 72 MPa, and the remaining parameters were chosen as listed in Table 4.

Figure 5 illustrates that the slope of the productivity curve of well L2-3 is 0.4 and the intercept is 2.72. According to Equation (5) for the exponential empirical method, $q_{AOF} = 289.84 \times 10^4 \text{ m}^3/\text{d}$ for well L2-3.

4.4. Results of Numerical Simulation Method. In this study, dynamic simulations of ultimate gas production were performed for the three gas wells based on the properties of the deep shale gas reservoirs in the Luzhou block as well as the wellbore parameters and production systems of the gas wells. The AOFs of the gas wells were obtained from the simulated inflow performance relationship (IPR) curves when the bottom-flow pressure was zero. The CH_4 content in the gas recovered from the three gas wells exceeded 98%, with extremely low amounts of CO_2 and N_2. The detailed input parameters of the model are listed in Table 5.

As shown in Figure 6, the intersection of an IPR curve with the x-axis is the AOF of the gas well. The results of the numerical simulation are very similar to those calculated by the pseudogas production index method and the water production index analytical method. Among them, well L2-3 has the highest AOF of $297.00 \times 10^4 \text{ m}^3/\text{d}$, whereas well Y2-8 has the lowest AOF of $110.00 \times 10^4 \text{ m}^3/\text{d}$.

4.5. Contrast and Verification. We compared the AOF results obtained using the various calculation methods. As shown in Figure 7, well L2-3 has the highest AOF, with an average of $278.1 \times 10^4 \text{ m}^3/\text{d}$. Well Y2-8 has the lowest AOF, with an average of $100.2 \times 10^4 \text{ m}^3/\text{d}$, whereas well Y4-5 has an average AOF of $142.4 \times 10^4 \text{ m}^3/\text{d}$.

By comparing the AOFs calculated by the different methods, Figure 7 shows that the results calculated using the water production index analytical method are small, which is caused by using the pressure square, instead of the pseudopressure. This is because the initial reservoir pressure in deep shale is high, typically greater than 40 MPa. However, as a gas well continues to produce, the pressure rapidly decreases to 20–30 MPa and subsequently remains stable. This suggests that a small portion of the pressure in the initial stages of gas production is overestimated by the analytical method. The accuracy of the analytical pseudogas production index method and water production index method for computing the AOFs is confirmed by the findings of the various approaches, which generally show minimal difference. In the absence of productivity test data, this study suggests that different methods should be used to calculate the AOFs for gas wells in different production stages. For gas wells in the flowback stage, the water production index analysis method is recommended, and for early gas-producing wells in the unstable flow stage, the pseudogas production index method is suggested to evaluate well productivity.

4.6. Results of EUR Evaluation Method. There are multiple ways to determine the EUR of gas wells, as explained in Section 3, and the results must be based on a thorough investigation of the fitting effects of various approaches. To better fit the dynamic production curves of shale gas wells, this study uses modern PDA methods to calculate the EUR, which mainly include the Blasingame, A-G, and NPI methods. The production curves of the three gas wells in the block exhibit good characteristics and are in the continuous or fluctuating decline stage, thus meeting the conditions for the modern PDA methods. This paper briefly describes the calculation process and presents the analysis and discussion of the calculation results.
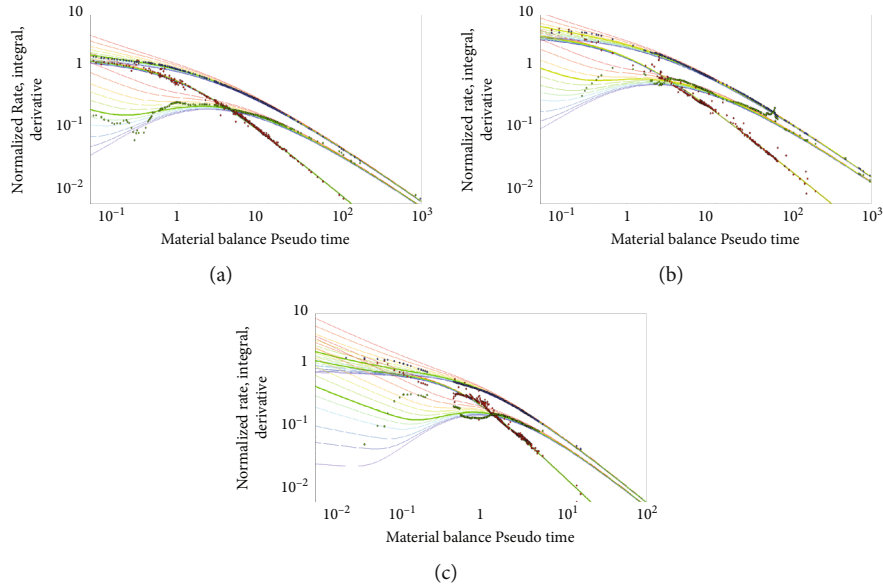
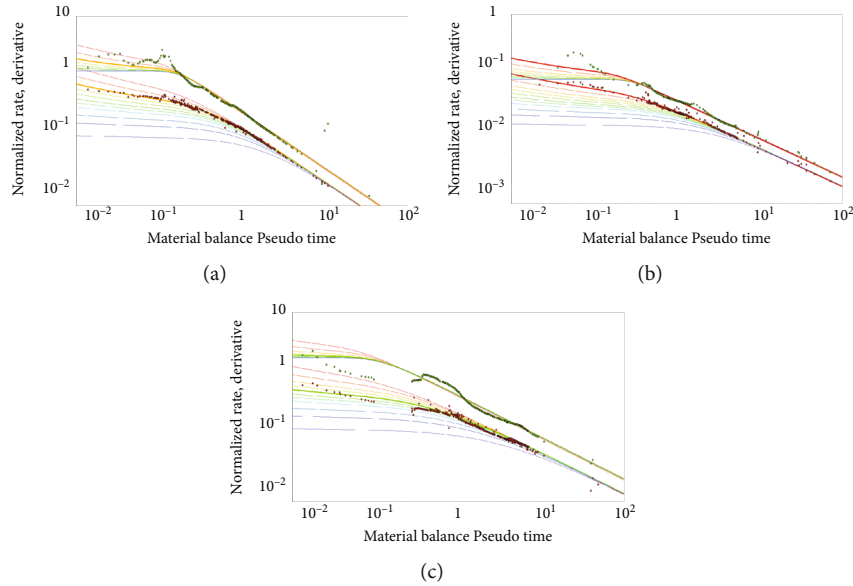Figure 8: Fitting of Blasingame method type curve and production data: (a) L2-3, (b) Y2-8, and (c) Y4-5.

Figure 9: Fitting of A-G method type curve and production data: (a) L2-3, (b) Y2-8, and (c) Y4-5.

4.6.1. Production Data Preprocessing. Shale gas well production data can show various incorrect data points, which are errors caused by on-site testing. In particular, data points near the times when a well is switched on and off typically have large errors, and researchers must manually filter and remove such erroneous information.

4.6.2. Calculation Parameters. Modern PDA methods mainly analyze gas production and wellhead tubing pressure, and the latter parameter needs to be converted using the wellbore tubular flow into the wellbore flow pressure for modification. In addition, various parameters such as the gas well temperature, initial reservoir pressure, net pay, porosity, and gas saturation are required, and the values of all parameters are listed in Table 6.

4.6.3. Fitting Type Curve and Calculating EUR. The pseudo-pressure-normalized production curve $(q_g/\triangle p_p)$, pseudo-pressure-normalized production integral curve $(q_g/\triangle p_p)_i$, and pseudo-pressure-normalized production derivative curve were obtained from the production data of the three gas wells. The three curves were fitted using the type curves of the Blasingame, A-G, and NPI methods. The results in Figures 8–10 show that the Blasingame method fits the data of L2-3 and Y4-5 the best, whereas the NPI method fits the data of Y2-8 the best.

As shown in Figures 8–10, the three shale gas wells reach the pseudostable flow stage, and the three methods are fitted well. Based on Figures 8(b) and 8(c) and 9(b) and 9(c), we conclude that, in the early unstable flow stage, the actual
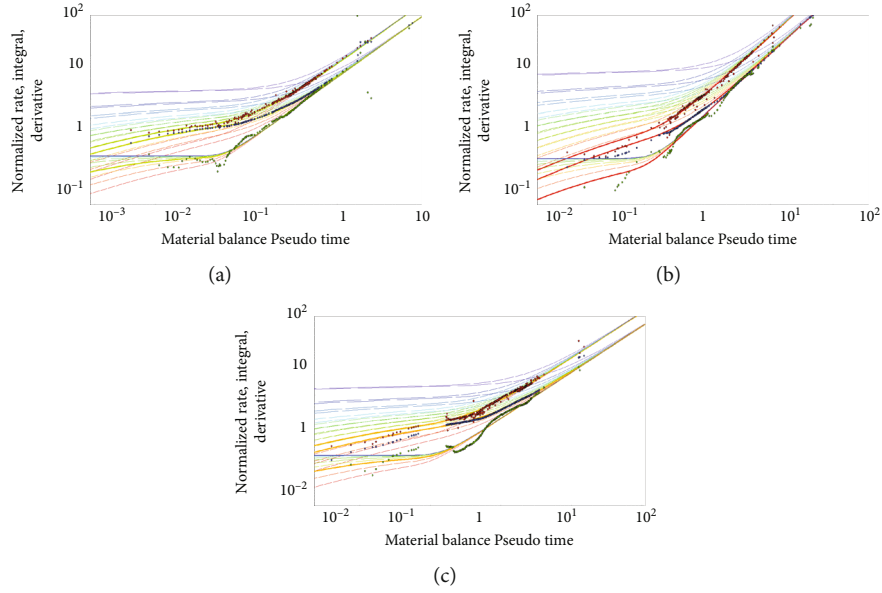
Figure 10: Fitting of NPI method-type curve and production data: (a) L2-3, (b) Y2-8, and (c) Y4-5.

Table 7: Calculation results of modern production decline analysis methods.

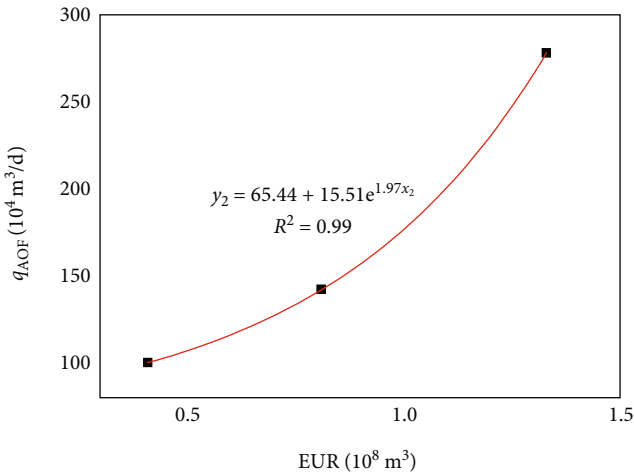| Well name | EUR (10^8 m^3) | | | | Average EUR (10^8 m^3) |
	Blasingame	A-G	NPI	FMB	
L2-3	1.33	1.26	1.25	1.21	1.26
Y2-8	0.44	0.43	0.41	0.41	0.42
Y4-5	0.81	0.97	0.94	0.84	0.89

Figure 11: Relationship curve between AOF and EUR of three gas wells.

production curves of Y2-8 and Y4-5 deviate slightly from the type curve, and the actual curves gradually approach the type curve downward. This suggests that the skin coefficients in the early stages of Y2-8 and Y4-5 gradually increase, and the fracturing fluid contaminates the surrounding gas wells,

which negatively affects the gas production and leads to a relatively lower AOF and EUR. From Figures 8(a) and 9(a), the gas production of well L2-3 is reliable and without contamination.

The EURs of the gas wells were calculated using a commercial software, and the results are provided in Table 7.

According to Table 7, the average EURs of L2-3 and Y2-8 are the highest and lowest at 1.26×10^8 m^3 and 0.42×10^8 m^3, respectively, while the average EUR of Y4-5 is 0.89 $\times 10^8$ m^3. The results demonstrate that the modern PDA methods are suitable for the gas wells in the block. A set of EUR evaluation processes for deep shale gas wells was proposed for this method, and the EURs of the three gas wells in the block were fitted and calculated. The calculation results presented some differences between the various methods, which indicates the uncertainty of the EUR evaluation. The Blasingame method is recommended for medium-to-high-production gas wells, and the NPI method is suggested for low-production wells. The A-G method does not fit well for the Luzhou deep shale gas well production data and is not recommended.

Based on the productivity evaluation results of the three shale gas wells in the block, the relationship curve between the AOF and EUR was drawn and obtained quantitatively, which is shown in Figure 11.

Based on the fitting results, this study concludes that the AOFs and EURs of the deep shale gas wells in the Luzhou block have a good exponential relationship and $R^2 = 0.99$. The error analysis of the calculated value of the model and the actual value is shown in Table 8.

This is because water production in the flowback stage effectively characterizes the initial productivity of the fracture system, and high water production implies good fracture development. The productivity of a shale gas well is determined by the original geological reserves and the fracture system's channel conductivity. There must be a quantitative

TABLE 8: Error analysis results.

Well name	Fitting model	EUR (10^8 m^3)	q_{AOF} (10^4 m^3/d) (model value)	q_{AOF} (10^4 m^3/d) (actual value)	Error analysis (%)
L2-3		1.26	270.3	278.1	2.81
Y2-8	$y_2 = 65.44 + 15.51e^{1.97x}{}_2$	0.42	100.32	100.2	0.12
Y4-5		0.89	139.4	142.4	2.11

relationship between initial productivity and the EUR. Theoretical analysis suggests that a high initial productivity of the fracture system implies a high EUR of a gas well. As a result, achieving optimal gas well development early on and achieving significant initial production productivity are critical issues for shale gas to effectively increase production. Geological and engineering factors influence both of these key parameters of production productivity evaluation. Furthermore, research on the dominant productivity control factors is the foundation for developing a model for high-production shale gas wells, which requires additional in-depth research.

5. Conclusion

AOF and EUR are critical parameters for assessing productivity. In this study, the productivity of three deep shale gas wells from the Luzhou block in the Sichuan Basin of China is calculated by using the established method. The utility and potential of the various methods are discussed and analyzed. The main conclusions of this study are as follows:

(1) A pseudogas production index method and a water production index analytical method are introduced in this study as new methods for calculating the AOF. The water production index analytical method only requires stable production data in the flowback stage to derive the AOF, which are simple to obtain, reducing the calculation costs and avoiding the calculation errors caused by multiple parameters. The results show that wells L2-3 and Y2-8 have the highest and lowest AOFs, averaging 278.1×10^4 m^3/d and 100.2×10^4 m^3/d, respectively, and the average AOF of well Y4-5 is 142.4×10^4 m^3/d. The AOF calculation methods for gas wells in different stages of production are different. The pseudogas production index method is recommended for gas wells in the early unstable flow stage. The water production index analytical method is suggested for gas wells in the flowback stage, These methods focus on the accuracy of the selected data, mainly including identification of the flow phase, pressure, gas production, water production, and time; otherwise, it will cause errors in the results

(2) The AOFs of the three shale gas wells are calculated using an exponential method and a numerical simulation method, and the results are comparable to those of the pseudogas production index method and the water production index analytical method. Consequently, the accuracies of the new methods and the enhancement of their reliability are confirmed

(3) The areas near the wellbores of Y2-8 and Y4-5 are contaminated with the fracturing fluid, which is detrimental to obtaining a high AOF and EUR. The EUR calculation results show that the average EUR of L2-3 is the highest at 1.26×10^8 m^3 and the lowest at 0.42×10^8 m^3. Based on the fitting results, the Blasingame method is recommended for medium-to-high-production gas wells, whereas the NPI method is suggested for low-production wells

(4) The AOFs and EURs of the gas wells have a strong exponential relationship and $R^2 = 0.99$. The AOF of a gas well characterizes the maximum productivity of the shale fracture system. The results suggest that the magnitude of gas production is proportional to the initial productivity of the fracture system. The original geological reserves and the fracture system channel conductivity are critical factors for determining whether a gas well is highly productive. A high initial productivity of the fracture system implies a high EUR of a single well

Appendix

A. Flowback Fluid Production Index of Analytical Method

Herein, we provide the derivation of the water production index analytical method for predicting the productivity of deep shale gas wells.

The following assumptions were made for the model formulation, which are explained subsequently:

(1) The reservoir is horizontal, infinite, and homogeneous with uniform thickness and constant porosity

(2) The analytical model is developed based on the flowback stage in Figure 2, considering the flowback process in the artificial fracture. The fluid is a single-phase microcompressible fluid with a constant compressibility coefficient and viscosity

(3) The shale gas well production analytical model assumes that the fluid is a single-phase compressible gas, μZ is a constant, and the pressure drop in the gas production stage is large and fast. Therefore, the pseudopressure is replaced by pressure squared p^2 in the differential equation

(4) The effects of shale gas desorption and diffusion are negligible

(5) Darcy's law dominates the fluid flow in the fracture. The entire flow process is isothermal

The derivation process is as follows:

For the flowback stage, the differential equation describing the fluid flow between the matrix and the fracture is expressed in Equation (A.1), where 0.0853 is the coefficient generated in the unit conversion process.

$$\frac{\partial^2 p}{\partial x^2} = \frac{\varphi \mu c_t}{0.0853k} \frac{\partial p}{\partial t}. \tag{A.1}$$

The boundary conditions are as expressed in

$$p(x, 0) = p_i, \tag{A.2}$$

$$\left(\frac{\partial p}{\partial x}\right)_{x \longrightarrow 0} = \frac{q_w B \mu}{0.0853 khwn}, \tag{A.3}$$

$$p(\infty, t) = p_i. \tag{A.4}$$

The dimensionless variable relationship is defined in

$$p_D = \frac{0.0853 kh(p_i - p)n}{q_w \mu B}, \tag{A.5}$$

$$t_D = \frac{0.0853 kt}{\phi \mu c_t w^2}, \tag{A.6}$$

$$x_D = \frac{x}{w}. \tag{A.7}$$

Substituting Equations (A.5)–(A.7) into Equation (A.1) yields a dimensionless differential equation, which is expressed in

$$\frac{\partial^2 p_D}{\partial x_D{}^2} = \frac{\partial p_D}{\partial t_D}. \tag{A.8}$$

The boundary conditions are as expressed in

$$p_D(x_D, 0) = 0, \tag{A.9}$$

$$\frac{\partial^2 p_D(0, t_D)}{\partial x^2} = -1, \tag{A.10}$$

$$p_D(\infty, t_D) = 0. \tag{A.11}$$

If $p_D(x_D, t_D) = m_D(x_D, t_D) \times x_D$, Equation (A.8) can be expressed as Equation (A.13).

$$\frac{\partial(x_D(\partial m_D/\partial x_D) + m_D(\partial x_D/\partial x_D))}{\partial x_D} = \frac{\partial m_D}{\partial t_D}, \tag{A.12}$$

$$\frac{\partial^2 m_D}{\partial x_D^2} + \frac{2}{x_D} \frac{\partial m_D}{\partial x_D} = \frac{\partial m_D}{\partial t_D}. \tag{A.13}$$

The boundary conditions are converted into

$$m_D(x_D, 0) = 0, \tag{A.14}$$

$$\left[x_D \frac{\partial m_D(x_D, t_D)}{\partial x_D} + m_D\right]_{x_D \longrightarrow 0} = -1, \tag{A.15}$$

$$m_D(\infty, t_D) = 0. \tag{A.16}$$

Taking $u = x_D/\sqrt{4t_D}$ yields

$$\frac{\partial u}{\partial x_D} = (4t_D)^{-1/2}, \tag{A.17}$$

$$\frac{\partial u}{\partial t_D} = \frac{1}{4} x_D t_D^{-3/2}, \tag{A.18}$$

$$\frac{\partial m_D}{\partial x_D} = \frac{\partial m_D}{\partial u} \frac{\partial u}{\partial x_D} = \frac{\partial m_D}{\partial u} (4t_D)^{-1/2}, \tag{A.19}$$

$$\frac{\partial^2 m_D}{\partial x_D^2} = \frac{\partial}{\partial x_D} \left(\frac{\partial m_D}{\partial u} \frac{\partial u}{\partial x_D}\right) = \frac{\partial}{\partial x_D} \left(\frac{\partial m_D}{\partial u} (4t_D)^{-1/2}\right)$$
$$= \frac{\partial}{\partial u} \left(\frac{\partial m_D}{\partial u} \frac{\partial u}{\partial x_D} (4t_D)^{-1/2}\right) = \frac{\partial^2 m_D}{\partial u^2} (4t_D)^{-1/2}, \tag{A.20}$$

$$\frac{\partial m_D}{\partial t_D} = \frac{\partial m_D}{\partial u} \frac{\partial u}{\partial t_D} = -\frac{1}{4} \frac{\partial m_D}{\partial u} x_D t_D^{-3/2}. \tag{A.21}$$

Substituting Equations (A.19)–(A.21) into Equation (A.13) yields

$$\frac{\partial^2 m_D}{\partial u^2} + \frac{2}{x_D} (4t_D)^{1/2} \frac{\partial m_D}{\partial u} = -\frac{\partial m_D}{\partial u} x_D t_D^{-1/2}. \tag{A.22}$$

Since $u = x_D/\sqrt{4t_D}$, Equation (A.22) can be converted to

$$\frac{d^2 m_D}{dx^2} + \left(\frac{2}{u} + 2u\right) \frac{dm_D}{du} = 0, \tag{A.23}$$

$$m_D(u \longrightarrow \infty) = 0, \tag{A.24}$$

$$\left[u \frac{dm_D}{du} + m_D\right]_{u \longrightarrow 0} = -1. \tag{A.25}$$

If $dm_D/du = m_D{}'$, Equation (A.23) can be converted into

$$\frac{dm_D{}'}{du} + \left(\frac{u}{2} + 2u\right) m_D{}' = 0, \tag{A.26}$$

$$\frac{1}{m_D{}'} dm_D{}' = -\left(\frac{2}{u} + 2u\right) du, \tag{A.27}$$

$$\ln m_D{}' + 2 \ln^u = -u^2 + c, \tag{A.28}$$

$$u^2 m_D{}' = e^{-u^2 + c}, \tag{A.29}$$

$$m_D{}' = C_1 \frac{e^{-u^2}}{u^2}, \tag{A.30}$$

$$m_D = C_1 \int_\infty^u \frac{e^{-u^2}}{u^2}\, du. \tag{A.31}$$

Substituting Equation (A.30) and Equation (A.31) into Equations (A.24) and (A.25) yields the integral constant, C_1, as expressed in Equation (A.33).

$$\lim_{u \to 0} C_1 u \frac{e^{-u^2}}{u^2} + C_1 \int_\infty^u \frac{e^{-u^2}}{u^2}\, du = -1, \tag{A.32}$$

$$C_1 = -\frac{1}{\sqrt{\pi}}. \tag{A.33}$$

By introducing an exponential integral function exp (x) and a complementary error function erfc (x), Equation (A.31) can be converted into

$$m_D = -\frac{1}{\sqrt{\pi}} \int_\infty^u \frac{e^{-u^2}}{u^2}\, du = \frac{1}{\sqrt{\pi}} \left(\frac{e^{-u^2}}{u} + 2\int_\infty^u e^{-u^2}\, du \right)$$
$$= \frac{1}{\sqrt{\pi}} \frac{e^{-u^2}}{u} - \text{erfc}\,(u). \tag{A.34}$$

Multiplying both sides of the equation by x_D yields

$$p_D(x_D, t_D) = x_D m_D = \frac{2\sqrt{t_D}}{\sqrt{\pi}} \exp\left(-\frac{x_D^2}{4t_D} \right) - x_D \,\text{erfc}\left(\frac{x_D}{2\sqrt{t_D}} \right). \tag{A.35}$$

When $x_D = 0$, the flowing bottom-hole pressure is obtained by

$$p_{wD}(t_D) = 2\sqrt{\frac{t_D}{\pi}}. \tag{A.36}$$

Equation (A.35) is subtracted from Equation (A.36) to yield

$$p_D(x_D, t_D) - p_{wD}(0, t_D) = \frac{2\sqrt{t_D}}{\sqrt{\pi}} \exp\left(-\frac{x_D^2}{4t_D} \right)$$
$$- x_D \,\text{erfc}\left(\frac{x_D}{2\sqrt{t_D}} \right) - 2\frac{\sqrt{t_D}}{\sqrt{\pi}}. \tag{A.37}$$

Substituting Equations (A.5)–(A.7) into Equation (A.37) yields

$$q_w = \frac{nhw(p_i - p_{wf})}{2B_w} \sqrt{\frac{0.0853\pi k\varphi c_t}{t\mu_w}}. \tag{A.38}$$

For the production stage, based on the same approach, a differential equation that can describe the shale gas flow between the matrix and fracture is established, which is expressed in

$$\begin{cases} \dfrac{\partial^2 m(p)}{\partial x^2} = \dfrac{\varphi\mu c_t}{k} \dfrac{\partial m(p)}{\partial t}, \\ m(x, 0) = p_i, \\ \left(\dfrac{\partial m}{\partial x} \right)_{x \to 0} = \dfrac{q_g \mu p_{sc} T}{0.0853 khwn T_{sc}}, \\ m(\infty, t) = p_i. \end{cases} \tag{A.39}$$

The obtained relationship between gas production and pseudopressure is expressed in

$$q_g = \frac{nhw(m(p_i) - m(p_{wf})) T_{sc}}{2p_{sc} T B_g} \sqrt{\frac{0.0853\pi k\varphi c_t}{t u_g}}. \tag{A.40}$$

Data Availability

Many thanks are due to the University of Chinese Academy of Sciences, PetroChina Research Institute of Petroleum Exploration and Development, and Institute of Porous Flow and Fluid Mechanics. The data used is production data from the Luzhou block in the Sichuan Basin of CNPC and is not publicly available.

Conflicts of Interest

The authors declare that they have no conflicts of interest.

Authors' Contributions

Yize Huang was responsible for conceptualization, methodology, software, and writing of an original draft. Xizhe Li assisted in funding acquisition and supervision. Wei Guo contributed to the resources and writing. Xiaohua Liu contributed to the resources and wrote, reviewed, and edited the manuscript. Wei Lin provided supervision and wrote, reviewed, and edited the manuscript. Chao Qian investigated and validated the study. Mengfei Zhou investigated and validated the study. Yue Cui investigated and validated the study. Xiaomin Shi investigated and validated the study.

Acknowledgments

References

[1] C. Zou, Q. Zhao, L. Cong et al., "Development progress, potential and prospect of shale gas in China," *Natural Gas Industry*, vol. 41, no. 1, pp. 1–14, 2021.

[2] X. Ma and J. Xie, "The progress and prospects of shale gas exploration and exploitation in southern Sichuan Basin, NW China," *Petroleum Exploration and Development*, vol. 45, no. 1, pp. 172–182, 2018.

[3] H. E. Zhiliang, N. I. Haikuan, and J. I. Tingxue, "Challenges and counter measures of effective development with large scale of deep shale gas in Sichuan Basin," *Reservoir Evaluation and Development*, vol. 11, no. 2, pp. 1–11, 2021.

[4] M. A. Xinhua, W. A. Hongyan, Z. H. Qun et al., ""Extreme utilization" development of deep shale gas in southern Sichuan Basin, SW China," *Petroleum Exploration and Development*, vol. 49, no. 6, pp. 1377–1385, 2022.

[5] M. A. Xinhua, L. I. Xizhe, F. Liang et al., "Dominating factors on well productivity and development strategies optimization in Weiyuan shale gas play, Sichuan Basin, SW China," *Petroleum Exploration and Development*, vol. 47, no. 3, pp. 594–602, 2020.

[6] H. Zhuang, *Dynamic Well Testing in Petroleum Exploration and Development*, Petroleum Industry Press, Beijing, 2009.

[7] X. Liu, F. Meng, Q. Li, Z. Guo, W. Shen, and C. Zhang, "Absolute open flow (AOF) potential evaluation for watered-out gas wells in water-drive gas reservoir," *Petroleum Science and Technology*, vol. 39, no. 7-8, pp. 249–269, 2021.

[8] J.-J. Arps and A. Smith, "Practical use of bottom-hole pressure buildup curves," in *Drill Production*, pp. 155–165, Practical. API, 1949.

[9] D. Ilk, J. A. Rushing, A. D. Perego, and T. A. Blasingame, *Exponential vs Hyperbolic Decline in Tight Gas Sands: Understanding the Origin and Implications for Reserve Estimates Using Arps' Decline Curves*, vol. 23, no. 4, 2008, Society of Petroleum Engineers, Denver, Colorado, USA, 2008.

[10] P.-P. Valko, "Assigning value to stimulation in the Barnett shale: a simultaneous analysis of 7000 plus production histories and well completion records," in *SPE hydraulic fracturing technology conference*, vol. 19no. 9, pp. 67–83, The Woodlands, Texas, 2009.

[11] A. Duong, "An unconventional rate decline approach for tight and fracture-dominated gas wells," *Society of Petroleum Engineers*, vol. 21, no. 6, pp. 23–34, 2010.

[12] A. Forrest, "Oil and gas reserves classification, estimation, and evaluation," *Journal of Petroleum Technology*, vol. 37, no. 3, pp. 373–390, 1985.

[13] R. Schilthuis, "Active oil and reservoir energy," *Transactions of the Aime*, vol. 118, no. 1, pp. 33–52, 1936.

[14] D. Havlena and A. Odeh, "The material balance as an equation of a straight line—part II, field cases," *Journal of Petroleum Technology*, vol. 16, no. 7, pp. 815–822, 1964.

[15] D. Havlena and A. Odeh, "The material balance as an equation of a straight line," *Journal of Petroleum Technology*, vol. 15, no. 8, pp. 896–900, 1963.

[16] L. Mattar and R. Mcneil, "The "flowing" gas material balance," *Journal of Canadian Petroleum Technology*, vol. 37, no. 2, pp. 52–65, 1998.

[17] J. Lee and R. Sidle, "Gas-reserves estimation in resource plays," *SPE Economics and Management*, vol. 2, no. 2, pp. 86–91, 2010.

[18] L. Mattar, D. Anderson, and G. Stotts, "Dynamic material balance—oil-or gas-in-place without shut-ins," *The Journal of Canadian Petroleum Technology*, vol. 45, no. 11, pp. 7–10, 2006.

[19] J. Arps, "Analysis of decline curves," *Transactions of the Aime*, vol. 160, no. 1, pp. 228–247, 1945.

[20] M. Fetkovich, "Decline curve analysis using type curves," *Journal of Petroleum Technology*, vol. 32, no. 6, pp. 1065–1077, 1980.

[21] D. Robert, "Type curves for finite radial and linear gas-flow systems: constant-terminal-pressure case," *Journal of Petroleum Technology*, vol. 25, no. 5, pp. 719–728, 1985.

[22] M. Fetkovich, M. E. Vienot, M. D. Bradley, and U. G. Kiesow, "Decline curve analysis using type curves: case histories," *SPE Journal*, vol. 2, no. 4, pp. 637–656, 1987.

[23] J. Palacio and T. Blasingame, "Unavailable-decline-curve analysis with type curves-analysis of gas well production data," in *SPE Annual Technical Conference and Exhibition*, pp. 121–134, Texas, USA, 1993.

[24] D. Ilk, A. D. Perego, J. A. Rushing, and T. A. Blasingame, *Integrating Multiple Production Analysis Techniques To Assess Tight Gas Sand Reserves: Defining a New Paradigm for Industry Best Practices*, 2008.

[25] D. Ilk, J. A. Rushing, A. D. Perego, and T. A. Blasingame, "Exponential vs. hyperbolic decline in tight gas sands: understanding the origin and implications for reserve estimates using Arps' decline curves," in *SPE Annual Technical Conference and Exhibition*, 2008.

[26] J. Krunal and J. Lee, "Comparison of various deterministic forecasting techniques in shale gas reservoirs," in *Unconventional Resources Technology Conference*, pp. 22–32, Denver, Colorado, USA, 2013.

[27] P. Valko and W. Lee, "A better way to forecast production from unconventional gas wells," in *SPE Annual Technical Conference and Exhibition*, pp. 19–22, Italy, 2010.

[28] S. Yu and D. Miocevic, "An improved method to obtain reliable production and EUR prediction for wells with short production history in tight/shale reservoirs," in *Unconventional Resources Technology Conference*, pp. 12–14, Denver, Colorado, USA, 2013.

[29] T. Patzek, F. Male, and M. Marder, "Gas production in the Barnett shale obeys a simple scaling theory," *Proceedings of the National Academy of Sciences of the USA*, vol. 110, no. 49, pp. 19731–19736, 2013.

[30] T. Blasingame, T. Mccray, and W. Lee, "Decline curve analysis for variable pressure drop/variable flowrate systems," in *SPE Gas Technology Symposium*, OnePetro, 1991.

[31] W. A. Jieming, L. I. Chun, S. U. Junchang et al., "An analysis method of injection and production dynamic transient flow in a gas field storage facility," *Petroleum Exploration and Development*, vol. 49, no. 1, pp. 179–190, 2022.

[32] M. Fetkovich and E. Fetkovich, "Useful concepts for decline forecasting reserve estimation and analysis," *SPE Reservoir Engineering*, vol. 11, no. 1, pp. 13–22, 1996.

[33] R. G. Agarwal, D. C. Gardner, S. W. Kleinsteiber, and D. D. Fussell, "Analyzing well production data using combined-type-curve and decline-curve analysis concepts," *SPE Reservoir Evaluation & Engineering*, vol. 2, no. 5, pp. 478–486, 1999.

[34] D. M. Anderson, G. W. Stotts, L. Mattar, D. Ilk, and T. A. Blasingame, "Production data analysis-challenges, pitfalls, diagnostics," in *SPE Annual Technical Conference and Exhibition*, San Antonio, Texas, 2006.

[35] J. Warren and P. Root, "The behavior of naturally fractured reservoirs," *SPE Journal*, vol. 3, no. 3, pp. 245–255, 1963.

[36] S. De, "Analytic solutions for determining naturally fractured reservoir properties by well testing," *SPE Journal*, vol. 16, no. 3, pp. 117–122, 1976.

[37] R. O. Bello and R. A. Wattenbarger, "Multi-stage hydraulically fractured horizontal shale gas well rate transient analysis," in *North Africa technical conference and exhibition*, Cairo, Egypt, 1988.

[38] M. Brown, E. Ozkan, R. Raghavan, and H. Kazemi, "Practical solutions for pressure-transient responses of fractured horizontal wells in unconventional shale reservoirs," *SPE Reservoir Evaluation & Engineering*, vol. 14, no. 6, pp. 663–676, 2011.

[39] E. Ozkan, R. Raghavan, and O. Apaydin, "Modeling of fluid transfer from shale matrix to fracture network," in *SPE Annual Technical Conference and Exhibition*, Texas, USA, 2010.

[40] I. Brohi, M. Pooladi-Darvish, and R. Aguilera, "Modeling fractured horizontal wells as dual porosity composite reservoirs-application to tight gas, shale gas and tight oil cases," in *SPE western north american region meeting*, Anchorage, Alaska, USA, 2011.

[41] E. Ozkan, M. Brown, R. Raghavan, and H. Kazemi, "Comparison of fractured-horizontal-well performance in tight sand and shale reservoirs," *SPE Reservoir Evaluation & Engineering*, vol. 14, no. 2, pp. 248–259, 2011.

[42] E. Stalgorova and L. Mattar, "Practical analytical model to simulate production of horizontal wells with branch fractures," in *SPE Canadian unconventional resources conference*, Calgary, Alberta, Canada, 2012.

[43] E. Stalgorova and L. Mattar, "Analytical model for history matching and forecasting production in multifrac composite systems," in *SPE Canadian Unconventional Resources Conference*, Calgary, Alberta, Canada, 2012.

[44] Y. Hongjun, Z. Ermeng, F. Jing, W. Lei, and Z. Huiying, "Production analysis of composite model of five regions for fracturedhorizontal wells in shale gas reservoirs," *Journal of Southwest Petroleum University (Science & Technology Edition)*, vol. 37, no. 3, p. 9, 2015.

[45] J. Zhang, S. Huang, L. Cheng et al., "Effect of flow mechanism with multi-nonlinearity on production of shale gas," *Journal of Natural Gas Science and Engineering*, vol. 24, pp. 291–301, 2015.

[46] D. Fan and A. Ettehadtavakkol, "Transient shale gas flow model," *Journal of Natural Gas Science and Engineering*, vol. 33, pp. 1353–1363, 2016.

[47] Y. Su, G. Sheng, W. Wang, Y. Yan, and X. Zhang, "A multimedia coupling flow model for shale gas reservoirs," *Natural Gas Industry*, vol. 36, no. 2, pp. 52–59, 2016.

[48] A. Liu, S. Liu, and G. Sang, "Characterizing gas-water transport behavior in tight shale and its application on the well productivity," in *SPE Annual Technical Conference and Exhibition*, Anaheim, California, USA, 2020.

[49] H. Behmanesh, C. R. Clarkson, S. H. Tabatabaie, and L. Mattar, "Effect of relative permeability on modeling of shale oil and gas production," in *SPE/AAPG/SEG Asia Pacific Unconventional Resources Technology Conference*, 2021.

[50] W. Wang, D. Fan, and H. Sun, "Productivity model and analysis of influence factors of staged multi-cluster fractured horizontal wells in shale gas reservoirs," *Science Technology and Engineering*, vol. 12, no. 4, pp. 44–55, 2015.

[51] O. David, M. Hasan, and M. Fraim, "An anomalous productivity model for naturally fractured shale gas reservoirs," in *SPE Kingdom of Saudi Arabia Annual Technical Symposium and Exhibition*, Saudi Arabia, 2017.

[52] Z. Sun, J. Shi, Z. Yang et al., "Evaluation about adsorption gas and free gas content inside shale matrix under a wide range of atmosphere conditions," in *ABU Dhabi International Petroleum Exhibition & Conference*, Abu Dhabi, 2019.

[53] J. Zeng, J. Liu, W. Li, Y. K. Leong, D. Elsworth, and J. Guo, "Shale shrinkage transition induced by the matrix-fracture equilibrium time lag: a neglected phenomenon in shale gas production," in *SPE/AAPG/SEG Asia Pacific Unconventional Resources Technology Conference*, 2021.

[54] F. Civan, "Effective correlation of apparent gas permeability in tight porous media," *Transport in Porous Media*, vol. 82, no. 2, pp. 375–384, 2010.

[55] T. Ali and J. Sheng, "Evaluation of the effect of stress-dependent permeability on production performance in shale gas reservoirs," in *SPE Eastern Regional Meeting*, OnePetro, 2015.

[56] D. U. Xianggang, H. U. Zhiming, G. A. Shusheng et al., "Shale high pressure isothermal adsorption curve and the production dynamic experiments of gas well," *Petroleum Exploration & Development*, vol. 45, no. 1, pp. 127–135, 2018.

[57] W. Li, J. Liu, J. Zeng, Y. K. Leong, and D. Elsworth, "A fully coupled multidomain and multiphysics model for shale gas production," in *5th ISRM Young Scholars' Symposium on Rock Mechanics and International Symposium on Rock Engineering for Innovative Future*, Okinawa, Japan, 2019.

[58] Q. Wang, Y. Hu, J. Zhao, L. Ren, C. Zhao, and J. Zhao, "Multiscale apparent permeability model of shale nanopores based on fractal theory," *Energies*, vol. 12, no. 17, p. 3381, 2019.

[59] B. Jia, J. Tsau, and R. Barati, "Investigation of shale-gas-production behavior: evaluation of the effects of multiple physics on the matrix," *SPE Reservoir Evaluation & Engineering*, vol. 23, no. 1, pp. 68–80, 2020.

[60] T. Wang, Q. Wang, J. Shi et al., "Productivity prediction of fractured horizontal well in shale gas reservoirs with machine learning algorithms," *Applied Sciences*, vol. 11, no. 24, article 12064, 2021.

[61] W. Niu, J. Lu, and Y. Sun, "Development of shale gas production prediction models based on machine learning using early data," *Energy Reports*, vol. 8, no. 4, pp. 1229–1237, 2022.

[62] H. Du, J. Jung, and S. Kwon, "Comparative study on supervised learning models for productivity forecasting of shale reservoirs based on a data-driven approach," *Applied Sciences*, vol. 10, no. 4, p. 1267, 2020.

[63] Y. Li, Z. Wang, Z. Pan, X. Niu, Y. Yu, and S. Meng, "Pore structure and its fractal dimensions of transitional shale: a cross-section from east margin of the Ordos Basin, China," *Fuel*, vol. 241, no. 2, pp. 417–431, 2019.

[64] Y. Li, J. Q. Chen, J. H. Yang, J. S. Liu, and W. S. Tong, "Determination of shale macroscale modulus based on microscale measurement: a case study concerning multiscale mechanical characteristics," *Petroleum Science*, vol. 19, no. 3, pp. 1262–1275, 2022.

[65] Y. Li, J. Chen, D. Elsworth, Z. Pan, and X. Ma, "Nanoscale mechanical property variations concerning mineral composition and contact of marine shale," *Geoscience Frontier*, vol. 13, no. 4, article 101405, 2022.

[66] L. Han, X. Li, W. Guo et al., "Characteristics and dominant factors for natural fractures in deep shale gas reservoirs: a case study of the Wufeng-Longmaxi formations in Luzhou Block, Southern China," *Lithosphere*, vol. 2022, no. 1, pp. 966–975, 2022.

[67] W. Lin, X. Li, Z. Yang et al., "Multiscale digital porous rock reconstruction using template matching," *Water Resources Research*, vol. 55, no. 8, pp. 6911–6922, 2019.

[68] W. Shen, Y. Xu, X. Li, W. Huang, and J. Gu, "Numerical simulation of gas and water flow mechanism in hydraulically fractured shale gas reservoirs," *Journal of Natural Gas Science and Engineering*, vol. 35, no. 9, pp. 726–735, 2016.

[69] L. I. Xizhe, L. I. Xiaohua, S. U. Yunhe et al., "Correlation between per-well average dynamic reserves and initial absolute open flow potential (AOFP) for large gas fields in China and its application," *Petroleum Exploration and Development*, vol. 45, no. 6, pp. 1088–1093, 2018.

[70] L. I. Hua, W. A. Weihong, and W. A. Yanyan, "Productivity characterization method of shale gas wells," *Reservoir Evaluation and Development*, vol. 9, no. 5, pp. 63–69, 2019.

[71] L. Xiaohua, Z. Chunmei, J. Yandong, and Y. Xifei, "Theory and application of modern production decline analysis," *Natural Gas Industry*, vol. 30, no. 5, pp. 50–54, 2010.

[72] J. E. Hodgin and D. R. Harrell, "The selection, application, and misapplication of reservoir analogs for the estimation of petroleum reserves," in *SPE Annual Technical Conference and Exhibition*, San Antonio, Texas, USA, 2006.

[73] W. Shen, T. Ma, X. Li, B. Sun, Y. Hu, and J. Xu, "Fully coupled modeling of two-phase fluid flow and geomechanics in ultra-deep natural gas reservoirs," *Physics of Fluids*, vol. 34, no. 4, pp. 043101–043151, 2022.

[74] W. Lee, "Modernization of the SEC oil and gas reserves reporting requirements," *SPE Economics & Management*, vol. 1, no. 1, pp. 4–10, 2009.

[75] J. Etherington, "Managing your business using integrated PRMS and SEC standards," *Society of Petroleum Engineers*, vol. 44, no. 6, pp. 33–44, 2009.

[76] R. Sidle and W. Lee, "An update on the use of reservoir analogs for the estimation of oil and gas reserves," *SPE Economics & Management*, vol. 2, no. 2, pp. 80–85, 2010.

[77] J. Guo, A. Jia, C. Jia et al., "Production laws of shale-gas horizontal wells," *Natural Gas Industry*, vol. 39, no. 10, pp. 53–58, 2019.

[78] Y. Wang, H. Liu, W. Wang, X. Hu, Y. Guo, and C. Dai, "Evaluation of shale gas well fracturing performance based on flowback water production data," *Petroleum Geology and Recovery Efficiency*, vol. 26, no. 4, pp. 125–131, 2019.

[79] H. Sun, G. Meng, W. Cao et al., "Applicable conditions of the binomial pressure method and pressure-squared method for gas well deliverability evaluation," *Natural Gas Industry*, vol. 7, no. 4, pp. 397–402, 2020.

[80] Z. Liu, Z. Pan, S. Li et al., "Study on the effect of cemented natural fractures on hydraulic fracture propagation in volcanic reservoirs," *Energy*, vol. 241, article 122845, 2022.

[81] N. Liu, M. Liu, and S. Zhang, "Flowback patterns of fractured shale gas wells," *Natural Gas Industry*, vol. 2, no. 2-3, pp. 247–251, 2015.

[82] T. Zhang, X. F. Li, Y. H. Wang et al., "Study on the effect of gas-shale reservoir special properties on the fracturing fluid recovery efficiency and production performance," *Natural Gas Geoscience*, vol. 28, no. 6, pp. 828–838, 2017.